IEEE Access
Multidisciplinary ⋮ Rapid Review ⋮ Open Access Journal

Received February 13, 2022, accepted March 8, 2022, date of publication March 11, 2022, date of current version March 23, 2022.

Digital Object Identifier 10.1109/ACCESS.2022.3158976

Machine Learning-Aided Design of Dielectric-Filled Slotted Waveguide Antennas With Specified Sidelobe Levels

TAREK NAOUS[1], (Student Member, IEEE), AMEN AL MERIE[2], SALWA K. AL KHATIB[2], (Student Member, IEEE), MOHAMMED AL-HUSSEINI[3], (Senior Member, IEEE), RAED M. SHUBAIR[4], (Senior Member, IEEE), AND HILAL M. EL MISILMANI[2], (Member, IEEE)

[1]Department of Electrical and Computer Engineering, American University of Beirut, Beirut 1107 2020, Lebanon
[2]Department of Electrical and Computer Engineering, Beirut Arab University, Beirut 1107 2809, Lebanon
[3]Beirut Research and Innovation Center, Lebanese Center for Studies and Research, Beirut 2052 6703, Lebanon
[4]Electrical and Computer Engineering Department, New York University (NYU), Abu Dhabi, United Arab Emirates

Corresponding author: Hilal M. El Misilmani (hilal.elmisilmani@ieee.org)

ABSTRACT This paper presents the use of machine learning (ML) to facilitate the design of dielectric-filled Slotted Waveguide Antennas (SWAs) with specified sidelobe level ratios (SLR). Conventional design methods for air-filled SWAs require the simultaneous solving of complex equations to deduce the antenna's design parameters, which typically requires further manual simulation-based optimization to reach the desired resonance frequency and SLR. The few works that investigated the design of filled SWAs, did not optimize the design for a specified SLR. For an accelerated design process in the case of specified SLRs, we formulate the design of dielectric-filled SWAs as a regression problem where based on input specifications of the antenna's SLR, reflection coefficient, frequency of operation, and relative permittivity of the dielectric material, the developed ML model predicts the filled SWA's design parameters with very low error. These parameters include the unified slots length and the non-uniform slot displacements required to achieve the desired performance. We experiment with several regressive ML algorithms and provide a comparative study of their results. Our numerical evaluations and validation experiments with the best performing ML models demonstrate the high efficiency of the proposed ML approach in estimating the dielectric-filled SWA's design parameters in only a few milliseconds. A comparison to the design obtained through conventional optimization using the Genetic Algorithm also indicates superiority of the ML models in computation time and resulting antenna performance.

INDEX TERMS Antenna design, slotted waveguide antennas, dielectric-filled SWA, sidelobe level ratio, machine learning, neural networks.

I. INTRODUCTION

Slotted waveguide antennas (SWAs) have been widely adopted in various radar, communications, and military applications due to their set of appealing characteristics [1]. These characteristics include simple design, relatively low weight, and small volume, high power handling capability, high efficiency, and good reflection coefficient [2]. SWAs are composed of rectangular waveguides with slot cuts made either on the broad wall or the narrow wall of the waveguide. The introduced slots are used to radiate energy from the antenna. Typical SWAs have rectangular-shaped slots but could also have elliptical or corner edge slots that provide enhanced power handling abilities [3], [4].

The design method for air-filled SWAs was first proposed by *Elliott* [5], [6] and *Stevenson et al. [7]*, which allowed the calculation of the design parameters of the antenna, including the slots length, width, displacements from the waveguide center-line, in addition to their distribution along the length of the waveguide [7]. The proposed method requires the

The associate editor coordinating the review of this manuscript and approving it for publication was Fulvio Schettino.

simultaneous solving of equations based on Stevenson equations and Babinet's principle [8]. The solution to these equations also relies on Stegen's assumption of the universality of the length of the resonant slots [9], in addition to Tai's formula [10] and Oliner's length adjustment factor [11]. While the aforementioned design approach provides good results, it is complex and relies on numerically solving various equations to deduce the antenna's design parameters, which typically requires further manual simulation-based optimization to reach the desired resonance frequency and Sidelobe Level Ratio (SLR). The need for manually optimizing the design of the SWA through simulations is another drawback, as it is very time-consuming.

An additional drawback of conventional SWAs is their narrow frequency range. Knowing that SWAs are made of rectangular waveguides, their sizes have to be enlarged when lower operating frequencies are desired, which can be a challenge when size is a limitation, especially since finding the required waveguide design parameters for the desired frequency range is not a straightforward procedure. In different situations, a limited choice of waveguides to be used as radiating SWAs exists, which sets some constraints on the operating frequency. A promising solution to the size and frequency range constraints faced in standard SWAs is the insertion of dielectric material inside the waveguide, without having to increase its size. The shift in the resonance frequency can be controlled by using dielectric materials with different relative permittivities to fill the SWAs. However, this requires extensive numerical computations and simulation-based optimization to find the right antenna design parameters and dielectric material properties for the desired frequency of operation and SLR.

It was first proposed by *Larson et al. [12]* that filling the SWA with a dielectric material can reduce the waveguide size needed, increase the flexibility in slots location, reduce the slot length that allows spacing the shunt slots entirely in the narrow wall, and prevent electrical breakdown when working with high power microwaves. Larson used Babinet's principle to modify the equations of the radiation resistance, guide wavelength, slots conductance, and slot resonant length for dielectric-filled SWAs, previously presented by *Elliott* and *Oliner* in [7], [11]. However, the modified equations are even more complex than the typical air-filled ones and rely on solving several equations with different parameters to reach the desired output. Moreover, the modified equations did not take into account the variations in the equations of slot displacements and were not used to design SWAs with specified side lobe ratios.

Since then, only a few works have been reported on the design of dielectric-filled SWAs, where, to our knowledge, no work investigated the design of filled SWAs for specified side lobe ratios, but rather most of the work analytically analyzed the dielectric-filled SWAs based on theoretical formulations and wave equations. Typically, a waveguide can be either fully filled [13], [14], partially filled [15], [16], or inhomogeneously filled [17]. Each type of these waveguides has its own design methods and modes of propagation. In [17] in-homogeneously filled waveguides with lossy dielectrics were analytically analyzed using a system of differential equations, transformed into a linear matrix eigenvalue problem. Partially filled SWAs with two slots and a dielectric slab have been also analytically analyzed using a hybrid full-wave technique in [18]. In [15] a mathematical model presenting a partially filled SWA has been analyzed, where it was shown that the insertion of the filling material increased the gain and expanded the operating range of the SWA when compared with air-filled SWAs. A partially-filled leaky-wave SWA with transverse slots has been analyzed to investigate the velocity factor, first null beamwidth, main beam, and the optimal antenna length dependencies for uniform filling and different slot lengths in [16]. Recently, partially and fully filled circularly polarized radial line slot arrays have been designed in [14] to improve the gain and radiation bandwidth. Improvements have been reported in the directivity and aperture efficiency of the antenna, but with sidelobe level ratios of 11 and 15 dB. The aim of this paper is to present a simplified and accelerated design approach of fully filled slotted waveguide antennas for specified sidelobe ratios. The design technique takes into account the desired resonance frequency, sidelobe level ratio, number of slots, and waveguide dimensions, to obtain the required slots length and non-uniform displacements.

In recent years, the field of antenna design and optimization has been appealing for the use of Machine Learning (ML) algorithms [19], [20], since most of the antenna structures that are of interest for real-world applications do not have closed-form solutions. In addition, the design of antennas and microwave devices often requires a laborious and time-consuming geometric parameter optimization process to achieve the desired target performance. The non-linear relationship between an antenna's geometric parameters and its operating frequency, return loss, and similar parameters, makes the design process more complex and computationally heavy, especially when the number of geometric parameters to optimize is many. To address this problem, many works in the literature have leveraged ML to develop reliable regression models that can predict optimal geometric parameters for target performance. As opposed to traditional design methods that rely on time-consuming electromagnetic simulations, trained ML models have very fast prediction time which can be leveraged for an accelerated design process. Hence, ML provides a computationally efficient way to estimate the antenna design parameters with low error and high speed.

The ML-based antenna design approach has been used to optimize the design of the fractal antenna and notch structure of MIMO systems [21], double T-shaped monopole antennas [22], square microstrip antennas with truncated corners [23], and many other types of antennas [24] and microwave components [25], [26]. Despite the extensive use of ML in the design of several antennas in the literature, a shortage exists in the application of ML to design SWAs. Only one related work is found in [27], where an ML

approach is used to optimize the length and the orientation angle of the coupling slots in a planar slotted waveguide antenna array. The SLR obtained is 13.5 dB. The model was trained using 189 data points collected through simulations in HFSS.

The objective of this work is to use ML to facilitate the design of dielectric-filled SWAs with specified sidelobe levels. Starting with an available waveguide of a given operating frequency range, the aim is to use this waveguide as an SWA but for a frequency lower than its nominal operating range, without having to replacing it with a larger one. For specified resonance frequency, SLR, and a permittivity of an available dielectric material, our proposed ML model is used to predict the length and the non-uniform displacements of the slots, required to achieve a desired sidelobe level, with low error, in a few milliseconds of computational time. The presence of such ML model allows for the very quick redesign of the filled SWA should the design parameters such as frequency and SLR change. In addition, the use of machine learning facilitates and speeds up the design/fabrication process. Sometimes, the fabrication process introduces some byproducts that lead to performance deterioration. To combat this, the design must be repeated to account for these fabrication issues. With the presence of an ML model of the antenna, the redesign process takes only a fraction of a second. New inputs are fed to the model and the outputs are just generated, which saves all the time needed for performing a new set of simulations.

To that end, this work's objectives are as follows:

- Develop a dataset of optimized design parameters (slot length and displacements) for various performance requirements (frequency of operation and SLR). The samples are obtained through conventional simulation-based optimization used to design dielectric-filled SWAs.
- Train several regressive ML algorithms in a supervised manner using the created dataset. The resulting ML models can approximate the geometric design parameters of filled SWAs given the desired frequency of operation and SLR.
- Numerically evaluate the performance of the developed models and provide a comparative analysis.
- Validate the performance of the best performing models by using their predictions to simulate the antenna and compare the resulting reflection coefficient and SLR to the ground-truth values in the test set.
- Conduct an error analysis on the validation results and highlight the strengths and shortcomings of the ML models.
- Compare with the results obtained through conventional optimization techniques such as the Genetic Algorithm.

The rest of the paper is organized as follows: The conventional design methodology of SWAs is presented in Section II, highlighting the challenges faced and motivating the need for adopting ML approaches in the case of dielectric-filled SWAs. Section III introduces our design approach SWAs filled with a dielectric material based on trained ML models. In Section IV, we analyze the performance of the developed ML models. A validation process is also presented for the best performing models, along with an error rate analysis and a verification for a design requirement. Concluding remarks are given in Section V.

II. CONVENTIONAL DESIGN METHODOLOGY OF SWAs

Based on the required resonance frequency, the waveguide inner dimensions, i.e. width and height, can be first found. Then, for the desired SLR and a total number of slots cut, the slots excitation are calculated from well-known distributions in discrete antenna arrays, e.g. Taylor and Chebyshev distributions. The air-filled SWA can be designed as detailed by *El Misilmani et al.* in [3], and summarized as follows:

- The first and last slots are separated by a distance of $m\lambda_g/4$ from both terminals, with m being an odd number, whereas consecutive slots are separated by $\lambda_g/2$.
- The slots lengths can be either non-uniform, for which the length of each slot is calculated based on optimization algorithms, or assumed to be uniform for simplicity purposes. Using the proposed closed-form equations in [3], the SWA resonant frequency did not vary when different displacements leading to different SLRs were applied, while assuming uniform slot length. For optimal radiation characteristics, the length of all slots is taken to be at their resonant length. For rectangular slots [7], this length is typically around 0.49λ. Because of the narrower ends of elliptical and round-ended slots, their length is expected to be slightly larger than $\lambda_0/2$, optimized through simulations for the round-ended slots used in this paper. Throughout the different designs that we have worked on using the proposed design procedure in this work, the modified round-ended slot length values differed from the typical rectangular slot lengths by 1% to 3% only.
- To achieve higher efficiency, the slots are placed in alternating order on the length of the waveguide.
- The slots can be displaced from the waveguide centerline by uniform or non-uniform displacements. In the uniform case, an SLR of around 13 dB can only be achieved, which is similar to the case of having equal excitations to discrete elements in an antenna array. For this, non-uniform displacements are used to achieve high SLR.

To show the difference between the design of air-filled SWA and dielectric-filled SWAs, the design equations of the slot displacements are provided in the following.

In the uniform case, the slot displacements are calculated as follows:

$$d_u = \frac{a}{\pi}\sqrt{\arcsin\left[\frac{1}{N \times G}\right]} \tag{1}$$

with N is the number of slots and:

$$G = 2.09 \times \frac{a}{b} \times \frac{\lambda_g}{\lambda_0} \times \left[\cos(0.464\pi \times \frac{\lambda_0}{\lambda_g}) - \cos(0.464\pi)\right]^2 \quad (2)$$

In the non-uniform case, the slot displacements are calculated as follows:

$$d_n = \frac{a}{\pi} \arcsin \sqrt{\frac{g_n}{2.09 \frac{\lambda_g}{\lambda_0} \frac{a}{b} \cos^2\left(\frac{\pi \lambda_0}{2\lambda_g}\right)}} \quad (3)$$

with $c_n s$ are the distribution coefficients that should be determined to achieve the desired SLR, and:

$$g_n = \frac{c_n}{\sum_{n=1}^{N} c_n}. \quad (4)$$

Equation (4) guarantees that $\sum_{n=1}^{N} g_n = 1$.

In filled waveguides, the cutoff frequency (f_c) of the waveguide can be decreased by the square root of the relative permittivity (ϵ_r) of the dielectric material that is filled inside the waveguide. For a fully filled rectangular SWA with dominant TE_{10} mode, the cutoff frequency can be calculated as follows:

$$(f_c)_{10} = \frac{c}{2a\sqrt{\mu_r \epsilon_r}} \text{ [Hz]} \quad (5)$$

As inspected from the design equations of the air-filled SWA, the different design parameters, including the slots length, positions, and displacements, all depend on the guide wavelength λ_g of the waveguide. This in turn will vary with the changes in the value of the dielectric constant of the filled material. However, using the design equations of the filled-SWAs do not result in optimized values of slots length and displacements required to operate the antenna at a desired resonance frequency and SLR. For this, a further manual optimization of dielectric-filled SWAs should be done that requires extensive analytical and simulation work. In this paper, we are proposing the use of ML to design this type of antenna, instead of the typical analytical formulations and optimization through simulations.

III. PROPOSED ML APPROACH FOR THE DESIGN OF DIELECTRIC-FILLED SWAs

A. PROBLEM DESCRIPTION

Let $X = [x_1, x_2, \ldots, x_{N_x}]$ denote our input feature vector where N_x is the number of features considered. Our inputs consist of $N_x = 4$ features that are namely: the relative permittivity ϵ_r of the dielectric material used to fill the SWA, the desired frequency of operation f_c, the desired value of the reflection coefficient s_{11} at f_c, and the desired value of the SLR. We note that ϵ_r is used as an input parameter since predicting its value would not be useful as the resulting predictions are continuous values that would defer from the available fixed and standardized values of ϵ_r to be used in the simulation software.

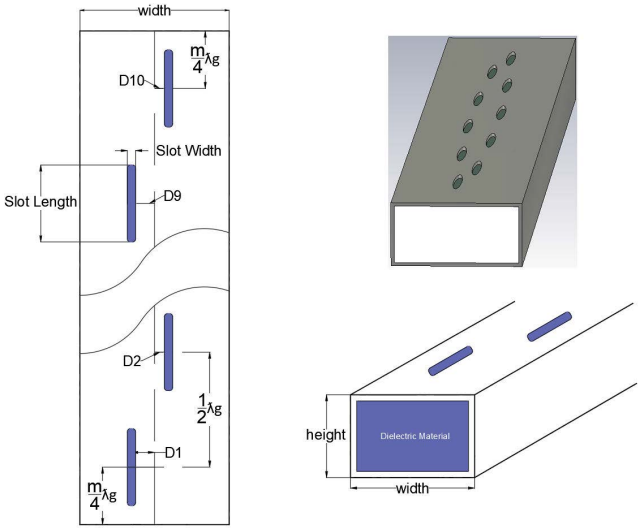

FIGURE 1. Sketch of the top and side views of the SWA with dielectric filling and 10 slots. The lengths of the slots are uniform while slot displacements are non-uniform.

Let $Y = [y_1, y_2, \ldots, y_{N_y}]$ denote our output feature vector containing the design parameters of the SWA to be predicted by the ML model. We consider $N_y = 6$ output design parameters: the slots length s_l and the displacements of the first five slots denoted by d_1, d_2, d_3, d_4, and d_5. We note that we do not include the rest of the displacement values in our output features since, when simulating the SWA, their values are taken to be equal to the first five displacements as such: $d_6 = d_5$, $d_7 = d_4$, $d_8 = d_3$, $d_9 = d_2$, and $d_{10} = d_1$.

The ML model we present in this paper is suitable for an SWA with 10 slots. To be able to design a filled SWA with a different number of slots, a new ML model has to be designed, for the sought number of slots. To do so, simulations for that specific number of slots have to be done, then the features and outputs from these simulations will be used to produce the new ML model. Once ready, this new ML model will be sufficient to estimate the characteristics of the antenna slots, even for cases that have not been included in the simulations. The results will be out in no time.

For the currently presented work, we apply several regressive ML models to learn the non-linear mapping from X to Y that can be then used for inference, allowing us to approximate the antenna design parameters without relying on tedious simulation-based optimization approaches. Four ML techniques are used: ANNs, Random Forest, Support Vector Regression (SVR), and the Least Absolute Shrinkage and Selection Operator (LASSO). In what follows, we provide mathematical descriptions of the techniques used and specify the set of hyper-parameters selected in each.

1) ARTIFICIAL NEURAL NETWORKS

ANNs, commonly referred to as neural networks, are modelled after how the human brain computes and processes

TABLE 1. Network hyperparameters.

Layers	Units	Activation	Parameters
Fully Connected 1	250	ReLU	1300
Fully Connected 2	200	ReLU	54810
Fully Connected 3	150	ReLU	31650
Fully Connected 4	100	ReLU	15100
Fully Connected 5	50	ReLU	5050
Fully Connected 6	6	Linear	306

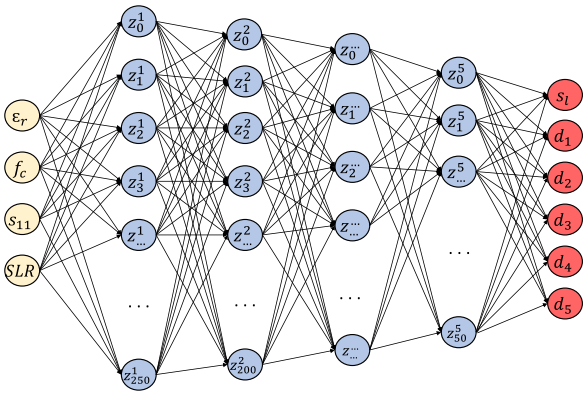

FIGURE 2. Architecture of the ANN used to predict the design parameters of the SWA.

information. They benefit from massively connected neurons which represent the computing units. The regular feed-forward operation in fully-connected ANNs is given by:

$$\begin{aligned} z_i^{l+1} &= w_i^{l+1} a^l + b_i^{l+1} \\ a_i^{l+1} &= g(z_i^{l+1}) \end{aligned} \tag{6}$$

where l represents the layer index, i represents the unit index, $\mathbf{z}$ is the input vector into a layer, $\mathbf{a}$ is the output vector from a layer, $\mathbf{w}$ is the weight parameter vector, $\mathbf{b}$ is the bias parameter vector, and g represents the chosen activation function. The network is trained to minimze the mean squared error as a loss function which is given by:

$$\mathcal{L}_{ANN} = \frac{1}{m} \sum_{i=1}^{m} (\hat{y}_i - y_i)^2 \tag{7}$$

where $\hat{y}_i$ is the prediction of the ANN and y_i is the ground-truth value of the i-th sample.

The architecture of the ANN we develop for SWA design optimization is illustrated in Fig. 2 and further described in Table 1 in terms of the number of layers, units, training parameters, and choice of activation. The network consist of an input layer that consist of the four input parameters. The input layer then feeds into several fully connected hidden layers with decreasing numbers of hidden units activated using the Rectified Linear Unit (ReLU) function. The final layer is a linear regressive layer that predicts the design parameters of the SWA. The specific number of neurons, in addition to the choice of activation used, was obtained via a process of hyper-parameter tuning for optimal performance on the validation set.

2) RANDOM FOREST

Random forest is an ensemble technique that averages the result of a collection of de-correlation decision trees. As trees are notoriously known to be noisy, averaging their results is beneficial in reducing variance. In random forest, multiple decision trees are fitted on randomly drawn bootstrap samples from the training dataset, where a subset of the initial input features are selected. The random forest model then averages the results of each decision tree to make a prediction. Given an input sample x, the prediction $\hat{y}$ by the random forest model is then computed through:

$$\hat{y} = \frac{1}{N} \sum_{i=1}^{N} T_i(x) \tag{8}$$

where N is the total number of decision trees which was chosen to be 100 with no maximum depth specified, and $T(.)$ represents a decision tree.

3) SUPPORT VECTOR REGRESSION

Inspired by the widely popular and effective Support Vector Machines (SVMs) classifier, SVR is a regression algorithm that is characterized by the use of kernels and the control of the margin. Although SVR is less popular than SVMs, it has proven to be an effective approach in estimating real-value functions. SVR fits a symmetrical tube of width $\epsilon > 0$ around the estimated function in a way such that absolute values of errors that fall below the ϵ threshold are ignored below and above the estimate. Considering the function to be estimated is non-linear, kernels are used to map the input into a higher dimensional space, referred to as the kernel space [28]. The loss function of the SVR algorithm is given by:

$$\mathcal{L}_{SVR}(w, b) = \frac{1}{2}|w|^2 + C \sum_{i=1}^{m} |w.\phi(x_i) + b - y_i|_\epsilon \tag{9}$$

where $\phi(.)$ is the transformation that maps inputs from the feature space to the kernel space, C is a regularization term, and $|.|_\epsilon$ is the ϵ-sensitive loss. As kernel for transformation, we use the widely adopted Gaussian Radial Basis Function kernel. Following a process of hyper-parameter optimization using Grid Search, the optimal values of ϵ and C were selected to be 0.001 and 50 respectively.

4) LASSO

The LASSO method integrates the mean-squared error and the L_1 penalty in a linear model. Using the L_1 penalty for regularization results in a sparse solution as some of the parameters w may reach a value of zero, which is why LASSO introduces an effect of feature selection. The loss function of the LASSO method is given by:

$$\mathcal{L}_{Lasso}(w, b) = \sum_{i=1}^{m} (wx_i + b - y_i)^2 + \lambda \sum_{i=1}^{N_x} |w_i| \tag{10}$$

where λ is the regularization parameter that and $\sum_{i=1}^{N_x} |w_i|$ is the L_1 penalty. After hyper-parameter tuning, the optimal value of λ was found as 0.00001.

TABLE 2. Ranges of the input parameters covered in the dataset.

Input Parameters	Minimum Value	Maximum Value
f_c (GHz)	1.08	2.51
ϵ_r	2.1	6.0
SLR (dB)	6.9	29.5
S_{11} (dB)	-51.5	-5.5

TABLE 3. Ranges of the output parameters covered in the dataset.

Output Parameters	Minimum Value	Maximum Value
s_l	49.75	89.7
d_1	0.88	4.74
d_2	1.27	6.98
d_3	1.64	9.37
d_4	1.904	11.33
d_5	2.033	12.48

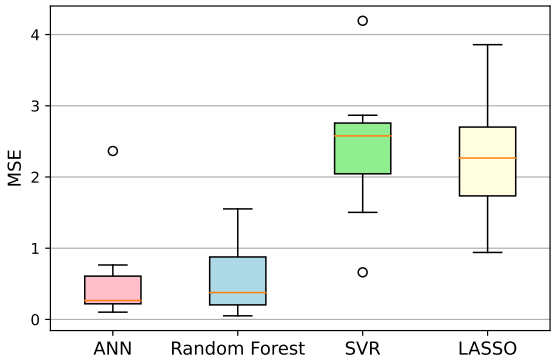

FIGURE 3. Boxplots showing the statistical summary of the models in terms of MSE after 10-fold cross validation.

B. DATASET GENERATION

To be able to train our proposed ML models, a dataset of 300 samples was generated by simulating a WR-284 SWA filled with dielectric material using the CST Microwave Studio software. Each sample in the dataset consists of the filled SWA's design parameters, which are the slots length, slot displacements value used have been optimized using the conventional design methodology using the conventional design methodology for various frequencies of operation and relative permittivity values of the dielectric material used for filling the SWA. The results obtained, in terms of reflection coefficient and SLR were then recorded. Table 2 and Table 3 display respectively the ranges of the various input and output parameters covered in the generated dataset.

IV. EXPERIMENTS & RESULTS

A. EXPERIMENTAL SETUP

We randomly partition the dataset into 80% training, 10% validation, and 10% testing using a random seed of 42. All models were developed, trained, and evaluated on the common data split. The ANN model is developed using the Tensorflow library [29] and trained using the adaptive moment estimation (ADAM) algorithm. The Random Forest, SVR, and LASSO models are developed and trained using the Scikit Learn library [30].

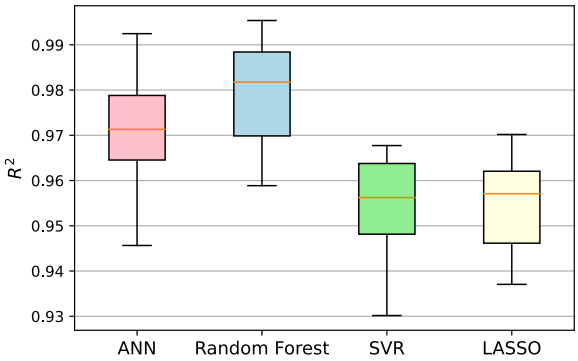

FIGURE 4. Boxplots showing the statistical summary of the models in terms of R^2 after 10-fold cross validation.

B. NUMERICAL EVALUATION

The performance of the models is evaluated using two statistical metrics widely adopted in the evaluation of regression models, which are the mean squared error (MSE) and the coefficient of determination, referred to as R^2 score [31]. The MSE of a model represents the average squared difference between the predicted outputs and the actual values. It is expressed by:

$$MSE = \frac{1}{m}\sum_{i=1}^{m}(h(x_i) - y_i)^2 \tag{11}$$

where m is the number of samples in the test set, $h(x_i)$ is the predicted output of the model, and y_i is the desired output which is the actual value in the test set.

The R^2 score is obtained by the following:

$$R^2 = 1 - \frac{\sum_{i=1}^{m}(h(x_i) - y_i)^2}{\sum_{i=1}^{m}(y_i - y_{mean})^2} \tag{12}$$

where y_{mean} represents the mean of the desired outputs in the test set.

1) CROSS-VALIDATION AND HYPOTHESIS SUMMARY STATISTICS

To evaluate the hypotheses of the obtained models, we perform 10-fold cross-validation and report the statistical summary of the MSE in the boxplots of Fig. 3. It can be noticed that the ANN achieves the best cross-validation results with a lowest median MSE of 0.238 and a small IQR of 0.219 to 0.607. The second-best performing model is the Random Forest which, compared to the ANN model, has a slightly higher MSE median of 0.313 and a larger IQR range of 0.204 to 0.877. Both ANN and Random Forest models outperform the SVR and the LASSO models, which showed worse cross-validation performance. The SVR and LASSO models showed high MSE medians and relatively larger Interquartile Ranges (IQRs) compared with the ANN and Random Forest models. Specifically, SVR achieved a median MSE of 2.714 and an IQR from 2.044 to 2.757, while the LASSO model had a slightly lower MSE median of 2.392 and an IQR of 1.734 to 2.701.

TABLE 4. Results achieved by the models on the test set for each output parameter and their average.

	Model	s_l	d_1	d_2	d_3	d_4	d_5	Average
MSE	ANN	0.98113	0.00427	0.00833	0.01402	0.02073	0.02254	0.17517
	Random Forest	0.49530	0.00597	0.01280	0.02270	0.03260	0.03895	0.10139
	SVR	8.94899	0.02076	0.042963	0.07179	0.09292	0.10717	1.54743
	Lasso	10.60835	0.02207	0.04521	0.07493	0.10073	0.11603	1.82789
R^2	ANN	0.98975	0.99345	0.99401	0.99427	0.99404	0.99455	0.99335
	Random Forest	0.99482	0.99084	0.99080	0.99072	0.99064	0.99059	0.99140
	SVR	0.90652	0.96819	0.96915	0.97068	0.97333	0.97413	0.96033
	Lasso	0.88919	0.96618	0.96753	0.96940	0.97108	0.97199	0.95590

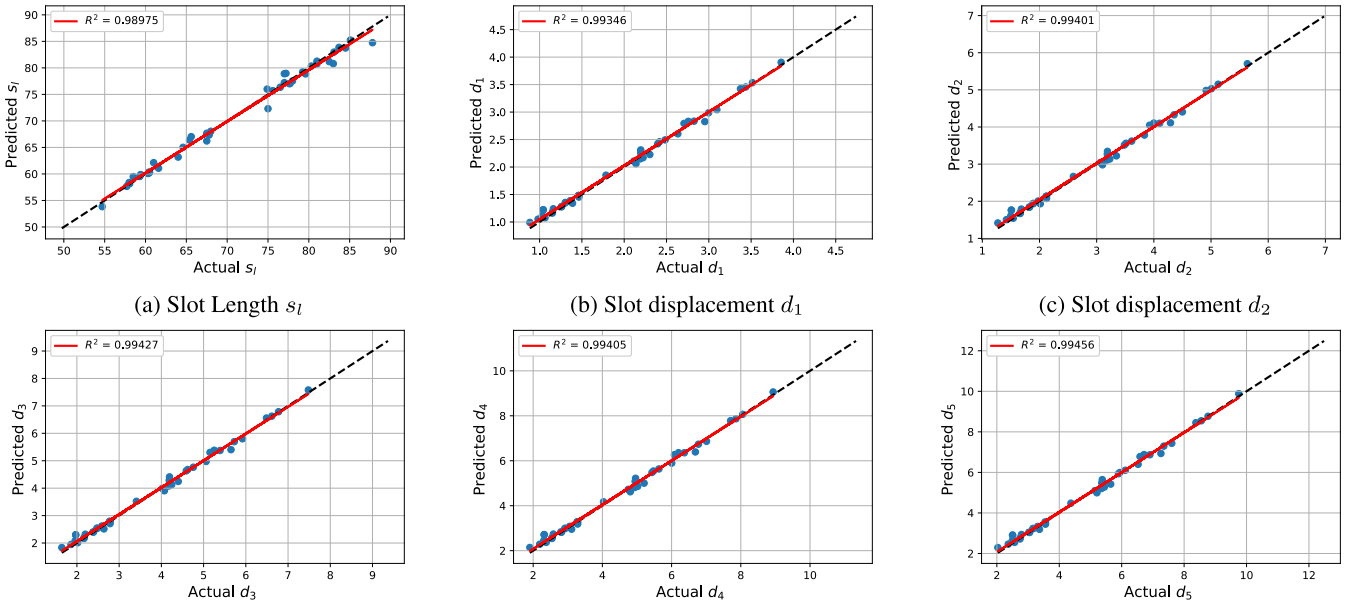

(a) Slot Length s_l (b) Slot displacement d_1 (c) Slot displacement d_2

(d) Slot displacement d_3 (e) Slot displacement d_4 (f) Slot displacement d_5

FIGURE 5. Comparative scatter plots of ANN model parameter predictions and their actual test set values.

Similar results are obtained in terms of R^2 score, as plotted in Fig. 4, where the ANN and Random Forest models also show superiority in performance compared with the SVR and LASSO models. In terms of R^2 score, the Random Forest achieves the best median value of 0.984 and an IQR of 0.969 to 0.988. The ANN model shows similar performance with a median R^2 score of 0.972 and had an IQR range of 0.964 to 0.978, which are very similar to the results of the Random Forest model. On the other hand, the SVR and LASSO models achieved lower median R^2 scores and smaller IQRs. The SVR model achieved a median R^2 score of 0.954 and an IQR of 0.948 to 0.963, while the LASSO model had very similar values with a median of 0.958 and an IQR of 0.946 to 0.962.

2) PERFORMANCE ON THE TEST SET

The results achieved by the ANN, Random Forest, SVR, and LASSO models on the test set in terms of MSE and R^2 are reported in Table 4. These test set results align with the observations in Fig. 3 and Fig. 4, where the ANN and Random Forest models outperformed the LASSO and SVR models that show high approximation errors. The Random Forest model achieved the best average MSE of 0.10139, while the ANN model achieved an average MSE of 0.17517. By inspecting the MSE values for each output design parameter, it can be noticed that the ANN model has lower MSE values for the slot displacements ($d1$ to $d5$), while the Random Forest model has a lower MSE value for the slot length s_l. In terms of R^2, a similar pattern in the results is observed. However, the differences in numerical scores of the ANN and Random Forest models are negligible, and thus they are both considered as high-performing models that can successfully approximate the mapping between the desired antenna characteristics and its design parameters with low error. The results achieved on the test set confirm the trend in results shown by the summary statistics reported after 10-fold cross-validation and highlight the superiority of the ANN over the rest of the models on the desired task. The numeric results achieved by the ANN model on the test also confirmed its ability to generalize to values outside the dataset with no signs of over-fitting to the training and validation sets.

Fig. 5 shows the correlation between the predicted values by the ANN model and the actual value in the test set for each of the output design parameters. Similar scatter plots for the Random Forest model are shown in Fig. 6. As it can be seen from the scatter plots of Fig. 5 and Fig. 6, the predictions by both the ANN and Random Forest models are very close to the actual values, with the points situated around

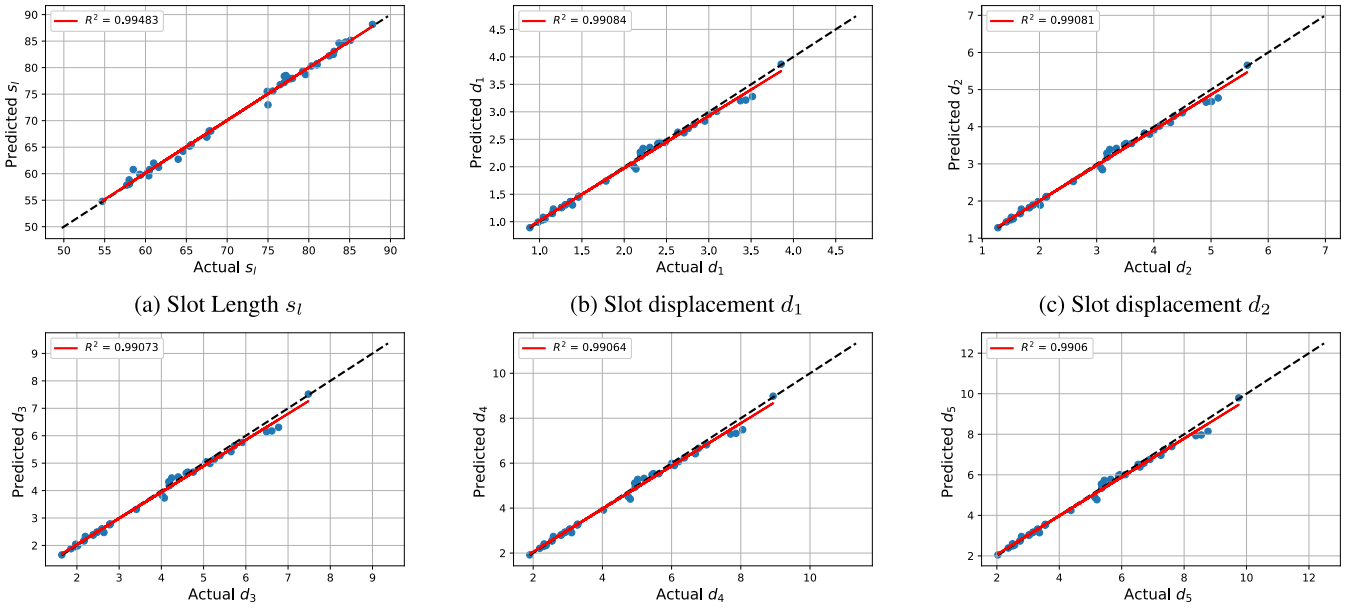

(a) Slot Length s_l (b) Slot displacement d_1 (c) Slot displacement d_2

(d) Slot displacement d_3 (e) Slot displacement d_4 (f) Slot displacement d_5

FIGURE 6. Comparative scatter plots of random forest model parameter predictions and their actual test set values.

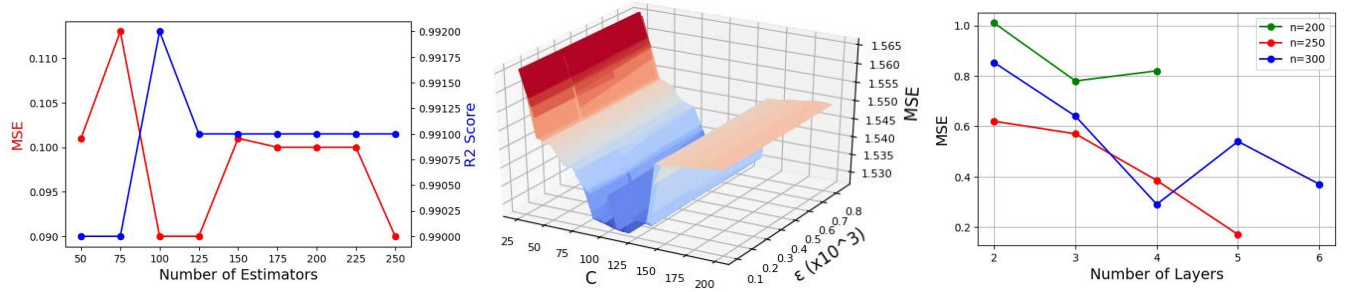

(a) Random Forest (b) SVR (c) ANN

FIGURE 7. Plots showing the influence of hyper-parameter tuning for the Random Forest (a), SVR (b), and ANN (c) models on the test set result. In (a), the optimal number of estimators in the Random Forest model is observed to be 100 where the highest R^2 score and lowest MSE value are achieved. In (b), the lowest MSE achieved by the SVR model is at a C value around 100 with no significant influence of ϵ. In (c), we show the resulting MSE for different architectures of the ANN model (in terms of layers and number of neurons). We select n neurons for the first layer and decrease it by 50 at each layer. It is noted that the last layer containing six neurons with linear activation are not counted. Thus, It can be observed that the optimal design is achieved with $n = 250$ and total number of layers equal to 5.

the identity line and an average R^2 score above 0.99 for both models. These plots demonstrate the high efficiency of the developed ANN and Random Forest models in predicting the design parameters of dielectric-filled SWAs given input design requirements.

Fig. 7 shows the influence of varying the hyper-parameters of the Random Forest, SVR, and ANN models and indicate how the optimal set of hyper-parameters were obtained.

C. VALIDATION AND ERROR RATE ANALYSIS

1) VALIDATION ON TEST SET EXAMPLES

To validate the effectiveness of the ANN and Random Forest models, we randomly select 3 samples from the test set and use the models at inference to predict the design parameters required. The predicted parameters, which are the slots length and slot displacements, are then used to simulate the dielectric-filled SWA using CST. We then compare in terms of S_{11} and SLR the output of the simulations obtained by using the design parameters predicted by the ANN and Random Forest models with the simulation outputs of the ground-truth test set values.

The results of this validation procedure are summarized in Table 5 for three different test samples that cover different values of the ϵ_r, the frequency of operation, and SLR. The error rate between the predicted design parameters and the simulation results are computed for each test sample. Fig. 8 shows the reflection coefficient plots and H-plane pattern plots for the results of the three different samples of Table 5.

For sample 1, the design parameters predicted by the ANN model are very close to the ground truth labels, with an error percentage ranging between 0.024% and 0.308%. Specifying these predicted design parameters in the simulator resulted in an S_{11} value of -10.5 dB at an operation frequency of 1.9 GHz and an SLR of 17.6 dB. These results are very

TABLE 5. Validation samples with ANN model design parameter predictions, test set ground truth values, and the obtained simulation outputs.

		Design Parameters							Simulator Output		
		s_l	d_1	d_2	d_3	d_4	d_5	ϵ_r	f_c	S_{11}	SLR
Sample 1	***Ground Truth***	60.5	2.484	3.612	4.757	5.635	6.117	2.85	1.9	-10	17.7
	ANN	60.314	2.493	3.620	4.763	5.636	6.106	2.85	1.9	-10.5	17.6
	Error (%)	0.308	0.4	0.222	0.146	0.024	0.169	-	-	4.761	0.568
	Random Forest	60.769	2.441	3.549	4.673	5.534	6.006	2.85	1.9	-8.72	18.2
	Error (%)	0.444	1.731	1.744	1.765	1.792	1.814	-	-	12.5	2.824
Sample 2	***Ground Truth***	63.0	2.293	3.331	4.383	5.187	5.627	3.4	1.68	-12.8	17.2
	ANN	62.945	2.308	3.340	4.402	5.205	5.629	3.4	1.68	-12.35	17.1
	Error (%)	0.087	0.649	0.269	0.431	0.345	0.035	-	-	3.643	0.584
	Random Forest	62.964	2.282	3.315	4.362	5.162	5.600	3.4	1.68	-12.357	17.4
	Error (%)	0.057	0.479	0.480	0.479	0.481	0.479	-	-	3.346	1.162
Sample 3	***Ground Truth***	75.6	1.465	2.123	2.785	3.286	3.559	4.5	1.32	-17.8	18.2
	ANN	75.7	1.481	2.134	2.776	3.266	3.529	4.5	1.32	-14	19.3
	Error (%)	0.132	1.116	0.552	0.322	0.6	0.835	-	-	27.142	5.699
	Random Forest	75.586	1.463	2.121	2.782	3.282	3.555	4.5	1.32	-17.027	19.6
	Error (%)	0.018	0.136	0.094	0.107	0.121	0.112	-	-	4.34	7.692

close to the ground-truth values where the error percentage is as low as 4.761% and 0.568% for the S_{11} and SLR values respectively. On the other hand, the Random Forest model's predictions showed slightly higher error percentages ranging from 0.444% to 1.792%, which resulted in a higher S_{11} error of 12.5% and SLR error of 2.824%. In this sample, the prediction error of the Random Forest model resulted in an S_{11} value below -10 dB, as shown in Fig. 8a, while the ANN model was able to provide design parameters that resulted in an S_{11} value that is very close to the ground truth value while satisfying the conditions for antenna resonance.

For sample 2, using the predicted design parameters of both ANN and Random Forest models resulted in S_{11} and SLR values which are very close to the ground-truth values. The ANN model predictions resulted in an S_{11} error of 3.643% and SLR error of 0.584% while the Random Forest model predictions resulted in an S_{11} error of 3.346% and SLR error of 1.162%. Both models were very successful in this sample in providing accurate design parameters which resulted in very close results to the ground-truth output as illustrated in Fig. 8c and Fig. 8d.

For sample 3, the ANN model resulted in an S_{11} error of 27.142% and an SLR error of 5.699% compared with the ground-truth values. The Random Forest model was able to provide a much lower S_{11} error at 4.34% but had a higher SLR error at 7.692%. While the ANN model resulted in a relatively high S_{11} error, the resulting S_{11} value of -14 dB is still enough for the antenna to achieve resonance, as shown in Fig. 8e, while providing a very close SLR value to the desired level as illustrated in Fig. 8f.

Based on these validation results, it can be concluded that the developed ANN and Random Forest models provide accurate predictions of the antenna's slot length and displacement parameters which do not surpass the 2% mark and that very closely match the ground truth values obtained through the conventional design methodology. However, even slight errors in the design parameters can cause a noticeable error in the resulting S_{11} values. In certain cases, such as the result of the Random Forest model in sample 1, the resulting error might not lead to a good resonance since the S_{11} will be slightly above -10 dB. However, this can be avoided by specifying an S_{11} requirement that is much lower than the resonance threshold, such as done in sample 3. In this manner, even with a relatively high S_{11} error percentage, the antenna will still achieve resonance and thus this would not affect performance. We also note that the resulting prediction error of the models can be further mitigated by enlarging the size of the dataset they were trained on, but which is a time-consuming process.

2) VALIDATION FOR A DESIGN REQUIREMENT

To further validate the effectiveness of our proposed ML-based design method, an additional example is provided here. Starting with a typical 10-slots SWA operating at 3 GHz, made of a WR-284 waveguide, the proposed method is used to decrease the resonance frequency of the SWA to 1.93 GHz, chosen arbitrarily outside the recommended frequency range of the WR-284 of 2.60 to 3.95 GHz. Typically, to reach this frequency, WR-510 or WR-430 waveguide can be used. However, both of these waveguides have larger dimensions than the WR-284, which requires changing the complete antenna system. Instead, we use our ML-based design method where the available WR-284 is filled with Arlon AD 295 dielectric material of a relative permittivity of 2.95, and the ANN model is used to predict the length and displacements of the slots required to decrease the resonance frequency to 1.93 GHz with an SLR of not less than 20 dB. The predicted slot length and displacements by the ANN model are listed in Table 6

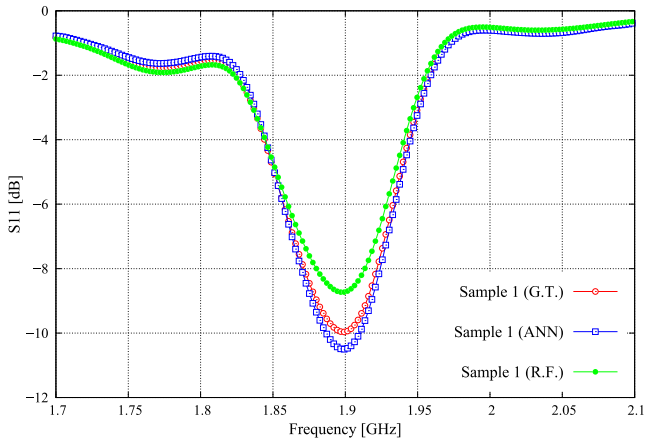

(a) Reflection coefficient plot for sample 1

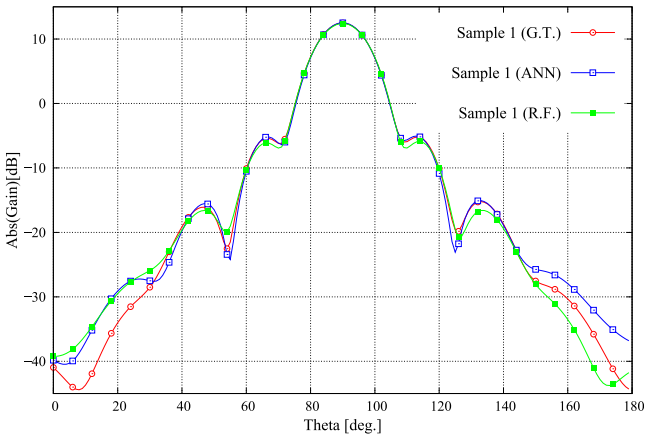

(b) H-plane pattern for sample 1

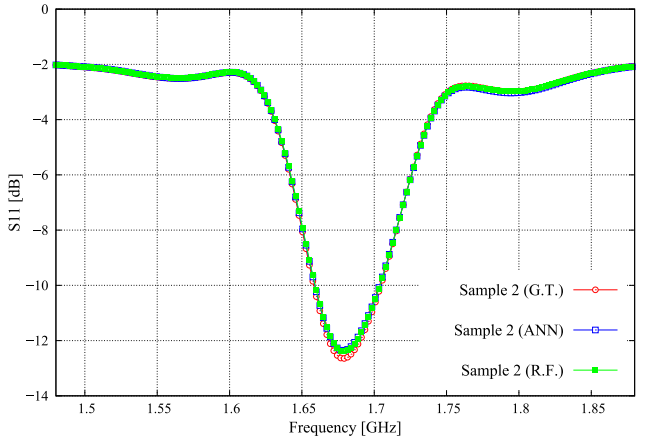

(c) Reflection coefficient plot for sample 2

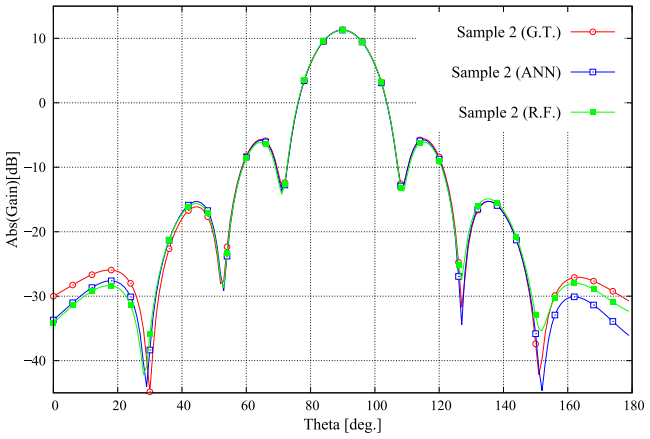

(d) H-plane pattern for sample 2

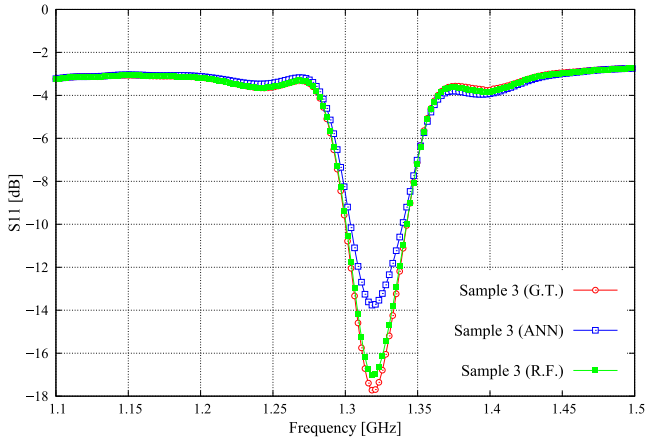

(e) Reflection coefficient plot for sample 3

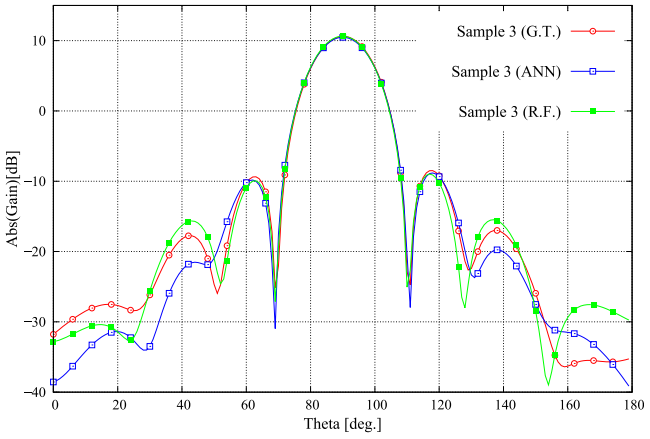

(f) H-plane pattern for sample 3

FIGURE 8. Antenna's reflection coefficient and H-plane pattern plots for each of the validation samples of Table 5. The plots show the simulation results of the antenna after using the design parameters predicted by the ANN and Random Forest models compared with the simulation results using the ground truth design parameters. G.T. stands for Ground Truth. R.F. stands for Random Forest.

and compared with those of the hollow SWA operating at 3 GHz.

Fig. 9 shows the simulated reflection coefficient results and gain pattern results in the H-plane respectively for both hollow SWA and filled SWA. Fig. 10 shows the gain pattern results in the H-plane respectively for the filled SWA designed using the ANN model. As can be observed in Fig. 9, using the predicted design parameters of the ANN model, the resonance frequency of the SWA was decreased from 3 GHz to 1.93 GHz, with a good value of reflection coefficient.

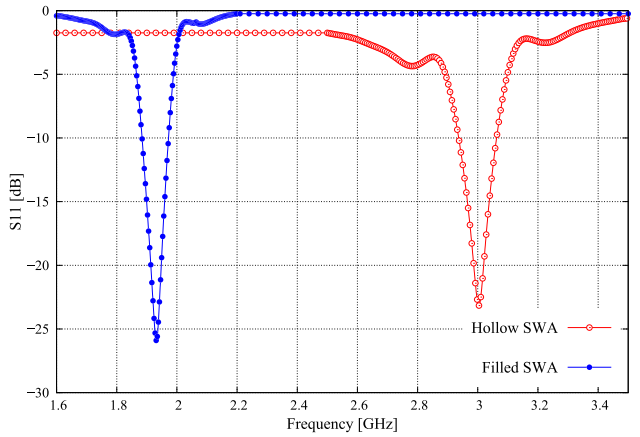

FIGURE 9. Comparative plot of the simulated reflection coefficients of the hollow SWA and the filled SWA designed using the ANN model.

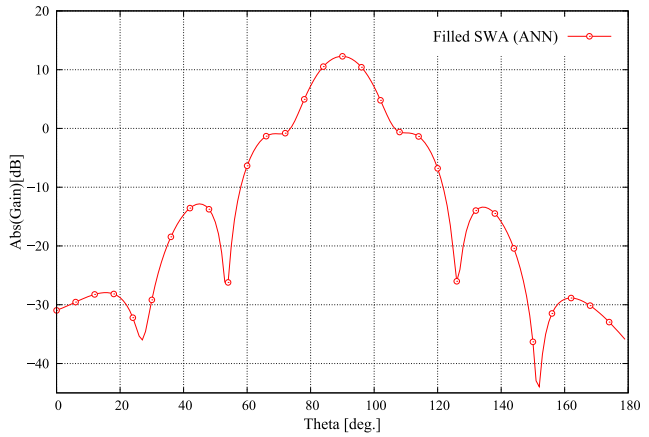

FIGURE 10. Gain pattern simulated results of the filled SWA designed using the ANN model.

TABLE 6. Design parameters of the hollow SWA and filled SWA. The filled SWA parameters are predicted by the ANN model to decrease the resonance of the antenna to 1.93 GHz.

	Design Parameters					
	s_l	d_1	d_2	d_3	d_4	d_5
Hollow SWA	51.7	4.526	6.65	8.903	10.737	11.796
Filled SWA	58.156	3.424	4.984	6.557	7.781	8.452

The SLR value has kept its value above 20 dB as required, as shown in Fig. 10. These results validate the effectiveness of our proposed method, which can be used to accurately predict design parameters required to lower the operational frequency of the SWA to the desired value, without having to resort to a waveguide of a larger size.

D. COMPUTATION TIME

In terms of computation time, the ANN model has a prediction time of around 0.0480 seconds while the Random Forest model has a prediction time of 0.0160 seconds. The computation time offered by both ANN and Random Forest models is a huge advantage over the conventional design methodology where optimization of the design parameters is required, a process that is heavily time-consuming and computationally expensive. Adopting conventional optimization algorithms for this task is very time consuming and may not converge to the optimal solution. We provide a comparison of the result obtained by the Genetic Algorithm optimizer in CST with the result of our ANN model for the following target: operation frequency of 2.31 GHz with $S_{11} = -20$ dB and $SLR = 25$ dB where a dielectric material with $\epsilon_r = 2.31$ is used. The optimization process using the Genetic Algorithm took 42 hours of continuous running to provide a result. Fig. 11 and Fig. 12 show the reflection coefficient and gain pattern plots of the designs obtained by both ANN model and Genetic Algorithm. It can be clearly observed that the resulting design by Genetic Algorithm-based optimization in CST fails to achieve resonance at the target frequency, which indicates that the conventional optimizer failed to converge to an optimal solution after a very large computation time. On the other hand, the predicted design by the ANN model, which is obtained in a few milliseconds, provides very good resonance with the S_{11} value reaching below -20 dB at the target frequency. This shows that the design process of dielectric-filled SWAs is rapidly accelerated by our proposed ML-based approach, where the prediction time of the ML models developed are leveraged. In addition, accurate design requirements are reached by adopting the ML-based

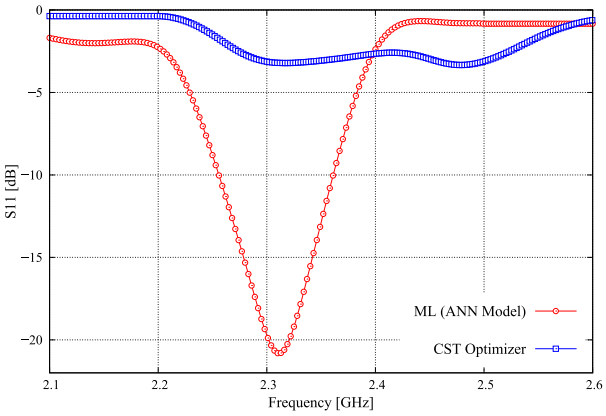

FIGURE 11. Comparative plot of the simulated reflection coefficients of the design obtained through the developed ANN model and the genetic algorithm-based optimization in CST.

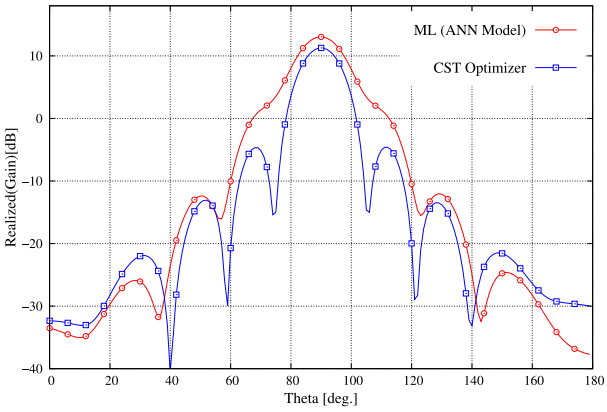

FIGURE 12. Realized gain pattern comparison plot of the design obtained through the developed ANN model and the genetic algorithm-based optimization in CST.

approach whereas perfect results may not be reached by conventional optimizers as shown in this example.

V. CONCLUSION

In this paper, an ML-based approach is used to design dielectric-filled SWAs for a desired SLR in an accelerated manner. Several developed ML models predict the required slots length and displacements for a specified resonance frequency, reflection coefficient value, and SLR. The results show the capability of the developed ML models to rapidly estimate the filled SWA design parameters with very low error. Validation and detailed analysis of the error rate were carried out, highlighting the effectiveness of the proposed ML-based design approach. In addition, the performance of the proposed ML-based design approach is compared to the result of Genetic Algorithm-based optimization in CST where superiority in both computation time and resulting antenna performance are shown. The availability of these ML models makes it possible to produce the design parameters of filled SWAs in milliseconds, and enables fast redesign when the inputs such as frequency of operation and SLR are changed.

REFERENCES

[1] N. Aboserwal, J. L. Salazar-Cerreno, and Z. Qamar, "An ultra-compact X-band dual-polarized slotted waveguide array unit cell for large E-scanning radar systems," *IEEE Access*, vol. 8, pp. 210651–210662, 2020.
[2] J. L. Volakis, *Antenna Engineering Handbook*. New York, NY, USA: McGraw-Hill, 2007.
[3] H. M. El Misilmani, M. Al-Husseini, and K. Y. Kabalan, "Design of slotted waveguide antennas with low sidelobes for high power microwave applications," *Prog. Electromagn. Res.*, vol. 56, pp. 15–28, 2015.
[4] H. M. El Misilmani, M. Al-Husseini, and K. Y. Kabalan, "Design procedure for planar slotted waveguide antenna arrays with controllable sidelobe level ratio for high power microwave applications," *Eng. Rep.*, vol. 2, no. 10, Oct. 2020, e12255.
[5] R. Elliott and L. Kurtz, "The design of small slot arrays," *IEEE Trans. Antennas Propag.*, vol. 26, no. 2, pp. 214–219, Mar. 1987.
[6] R. Elliott, "An improved design procedure for small arrays of shunt slots," *IEEE Trans. Antennas Propag.*, vol. 31, no. 1, pp. 48–53, Jan. 1983.
[7] A. F. Stevenson, "Theory of slots in rectangular wave-guides," *J. Appl. Phys.*, vol. 19, no. 1, pp. 24–38, 1948.
[8] H. G. Booker, "Slot aerials and their relation to complementary wire aerials (Babinet's principle)," *J. Inst. Elect. Eng., IIIA, Radiolocation*, vol. 93, no. 4, pp. 620–626, 1946.
[9] R. J. Stegen, "Longitudinal shunt slot characteristics," Res. Develop. DIV, Hughes Aircraft, Culver City CA, USA, Tech. Rep. Memo. 261, 1951.
[10] C. T. Tai, "Characteristics of linear antenna elements," in *Antenna Engineering Handbook*. New York, NY, USA: McGraw-Hill, 1961, pp. 3–8.
[11] A. A. Oliner, "The impedance properties of narrow radiating slots in the broad face of rectangular waveguide: Part I–Theory," *IRE Trans. Antennas Propag.*, vol. 5, no. 1, pp. 4–11, 1957.
[12] R. W. Larson and V. M. Powers, "Slots in dielectrically loaded waveguide," *Radio Sci.*, vol. 1, no. 1, pp. 31–35, Jan. 1966.
[13] J. Liu, D. R. Jackson, and Y. Long, "Modal analysis of dielectric-filled rectangular waveguide with transverse slots," *IEEE Trans. Antennas Propag.*, vol. 59, no. 9, pp. 3194–3203, Sep. 2011.
[14] N. Y. Koli, M. U. Afzal, K. P. Esselle, and M. Z. Islam, "Comparison between fully and partially filled dielectric materials on the waveguide of circularly polarised radial line slot array antennas," in *Proc. Int. Workshop Antenna Technol. (iWAT)*, Feb. 2020, pp. 1–3.
[15] N. Blinova, A. Lyakhovsky, and L. Yatsuk, "Multielement systems of slots in waveguides with partial dielectric filling," in *Proc. 3rd Int. Conf. Ultrawideband Ultrashort Impulse Signals*, Sep. 2006, pp. 229–231.
[16] R. R. Abdullin, Y. E. Mitelman, and S. N. Shabunin, "Radiation pattern of leaky-wave antenna based on partially-filled rectangular waveguide," in *Proc. Loughborough Antennas Propag. Conf. (LAPC)*, Nov. 2014, pp. 516–518.
[17] E. Silvestre, M. A. Abian, B. Gimeno, A. Ferrando, M. V. Andres, and V. E. Boria, "Analysis of inhomogeneously filled waveguides using a bi-orthonormal-basis method," *IEEE Trans. Microw. Theory Techn.*, vol. 48, no. 4, pp. 589–596, Apr. 2000.
[18] B. Zheng, Z. Shen, and G. Wen, "Full-wave analysis of dielectric-loaded waveguide slot antennas including internal and external mutual coupling," in *Proc. Asia–Pacific Microw. Conf.*, vol. 4, Dec. 2005, p. 4.
[19] H. M. E. Misilmani and T. Naous, "Machine learning in antenna design: An overview on machine learning concept and algorithms," in *Proc. Int. Conf. High Perform. Comput. Simulation (HPCS)*, Jul. 2019, pp. 600–607.
[20] C. Maeurer, P. Futter, and G. Gampala, "Antenna design exploration and optimization using machine learning," in *Proc. 14th Eur. Conf. Antennas Propag. (EuCAP)*, Mar. 2020, pp. 1–5.
[21] J. Nan, H. Xie, M. Gao, Y. Song, and W. Yang, "Design of UWB antenna based on improved deep belief network and extreme learning machine surrogate models," *IEEE Access*, vol. 9, pp. 126541–126549, 2021.
[22] Y. Sharma, H. H. Zhang, and H. Xin, "Machine learning techniques for optimizing design of double T-shaped monopole antenna," *IEEE Trans. Antennas Propag.*, vol. 68, no. 7, pp. 5658–5663, Jul. 2020.
[23] Z. Wang, S. Fang, Q. Wang, and H. Liu, "An ANN-based synthesis model for the single-feed circularly-polarized square microstrip antenna with truncated corners," *IEEE Trans. Antennas Propag.*, vol. 60, no. 12, pp. 5989–5992, Dec. 2012.
[24] H. M. El Misilmani, T. Naous, and S. K. Al Khatib, "A review on the design and optimization of antennas using machine learning algorithms and techniques," *Int. J. RF Microw. Comput.-Aided Eng.*, vol. 30, no. 10, Oct. 2020, Art. no. e22356.
[25] J. Jin, C. Zhang, F. Feng, W. Na, J. Ma, and Q.-J. Zhang, "Deep neural network technique for high-dimensional microwave modeling and applications to parameter extraction of microwave filters," *IEEE Trans. Microw. Theory Techn.*, vol. 67, no. 10, pp. 4140–4155, Oct. 2019.
[26] G. Pan, Y. Wu, M. Yu, L. Fu, and H. Li, "Inverse modeling for filters using a regularized deep neural network approach," *IEEE Microw. Wireless Compon. Lett.*, vol. 30, no. 5, pp. 457–460, Apr. 2020.
[27] J. Tak, A. Kantemur, Y. Sharma, and H. Xin, "A 3-D-printed W-band slotted waveguide array antenna optimized using machine learning," *IEEE Antennas Wireless Propag. Lett.*, vol. 17, no. 11, pp. 2008–2012, Nov. 2018.
[28] M. Awad and R. Khanna, "Support vector regression," in *Efficient Learning Machines*. Berkeley, CA, USA: Apress, 2015, pp. 67–80.
[29] M. Abadi, P. Barham, J. Chen, Z. Chen, A. Davis, J. Dean, and M. Devin, "Tensorflow: A system for large-scale machine learning," in *Proc. 12th USENIX Symp. Operating Syst. Design Implement. (OSDI)*, 2016, pp. 265–283.
[30] F. Pedregosa, G. Varoquaux, A. Gramfort, V. Michel, B. Thirion, and O. Grisel, "Scikit-learn: Machine learning in Python," *J. Mach. Learn. Res.*, vol. 12 no. 10, pp. 2825–2830, 2012.
[31] P. Harrington, *Machine Learning in Action*. Shelter Island, NY, USA: Manning, 2012.

TAREK NAOUS (Student Member, IEEE) received the B.E. degree in communications and electronics engineering from Beirut Arab University in June 2020. He is currently pursuing the M.E. degree in electrical and computer engineering with the American University of Beirut (AUB). He is also a Graduate Research Assistant at the Machine Intelligence Development Laboratory. His research interests include machine learning and natural language processing.

AMEN AL MERIE was born in Sidon, Lebanon, in 1994. He received the B.E. degree in communications and electronics engineering from Beirut Arab University (BAU), Lebanon, in 2018, and the M.E. degree from Beirut Arab University (BAU), in 2020. His research interest includes the design of filled slotted waveguide antennas.

SALWA K. AL KHATIB (Student Member, IEEE) is currently pursuing the B.E. degree in computer engineering with Beirut Arab University (BAU). She is also an Undergraduate Research Assistant at the Radio Frequency and Antenna Design Research Laboratory, BAU, where she is applying her expertise in machine learning to problems in antenna design optimization and breast tumor detection and localization from scattering parameters in microwave imaging. Since September 2019, she has been serving as the IEEE Student Branch Chairperson at the Faculty of Engineering. Her research interests include machine learning and computer vision.

MOHAMMED AL-HUSSEINI (Senior Member, IEEE) received the Ph.D. degree in electrical and computer engineering from the American University of Beirut (AUB), Beirut, Lebanon, in 2012. In 2013, he was a Visiting Researcher with The University of New Mexico, Albuquerque, NM, USA. He is currently a Co-Founder and the Research Program Director with the Beirut Research and Innovation Center (BRIC), Beirut, and a Lecturer with AUB. He has published five book chapters and over 100 papers in refereed journals and conference proceedings. His current research interests include material characterization, application of machine learning in electromagnetics and communications, cognitive radio, antenna design, and RF circuits. He was a recipient of the Dar Al-Handasah Ph.D. Fellowship from AUB.

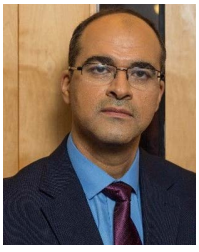

RAED M. SHUBAIR (Senior Member, IEEE) received the B.Sc. degree (Hons.) in electrical engineering from Kuwait University, Kuwait, in June 1989, and the Ph.D. degree (Hons.) in electrical engineering from the University of Waterloo, Waterloo, ON, Canada, in February 1993.

He was a Full Professor of electrical engineering with Khalifa University (formerly, Etisalat University College), UAE, from 1993 to 2017, during which he received several times the Excellence in Teaching Award and the Distinguished Service Award. He is currently a Senior Advisor at the Office of Undersecretary for Academic Affairs, Ministry of Education, United Arab Emirates. He is also a Full Professor of electrical engineering and the Chair of IEEE at New York University (NYU) Abu Dhabi. He has over 380 publications in the form of articles in peer-reviewed journals, papers in refereed conference proceedings, book chapters, and U.S. patents. His publication span several research areas, including 6G and terahertz communications, modern antennas and applied electromagnetics, signal and array processing, machine learning, the IoT and sensor localization, medical sensing, and nano-biomedicine. His current and past academic and research appointments also include the Massachusetts Institute of Technology (MIT), Harvard University, and the University of Waterloo. He is a fellow of the MIT Electromagnetics Academy and a Founding Member of MIT Scholars of the Emirates. He is a Board Member of the European School of Antennas, the Regional Director of the IEEE Signal Processing Society in IEEE Region 8 Middle East. He is a standing member of the editorial boards of several international journals and serves regularly on the steering, organizing, and technical committees for IEEE flagship conferences in antennas, communications, and signal processing, including several editions of IEEE AP-S/URSI, EuCAP, IEEE GloablSIP, IEEE WCNC, and IEEE ICASSP. He was a recipient of several international awards, including the Distinguished Service Award from ACES Society and MIT Electromagnetics Academy. He delivered more than 60 invited speaker seminars and technical talks in world-class universities and flagship conferences. He served as an invited speaker with the U.S. National Academies of Sciences, Engineering, and Medicine Frontiers Symposium. He has served as the TPC Chair for IEEE MMS2016 and IEEE GlobalSIP 2018 Symposium on 5G Satellite Networks. He holds several leading roles in the international professional engineering community. He served as the Founding Chair for the IEEE Antennas and Propagation Society Educational Initiatives Program. He is an Editor of the IEEE JOURNAL OF ELECTROMAGNETICS, RF, AND MICROWAVES IN MEDICINE AND BIOLOGY and the IEEE OPEN JOURNAL OF ANTENNAS AND PROPAGATION. He is a Founding Member of five IEEE society chapters in UAE, which are IEEE Communication Society Chapter, IEEE Signal Processing Society Chapter, IEEE Antennas and Propagation Society Chapter, IEEE Microwave Theory and Techniques Society Chapter, and IEEE Engineering in Medicine and Biology Society Chapter. He is the Founder and the Chair of IEEE at New York University Abu Dhabi. He is an Officer of the IEEE ComSoc Emerging Technical Initiative (ETI) on Machine Learning for Communications. He is the Founding Director of the IEEE UAE Distinguished Seminar Series Program for which he was selected to receive, along with Mohamed AlHajri of MIT, the 2020 IEEE UAE Award of the Year. He received the University of Waterloo Distinguished Doctorate Dissertation Award from the University of Waterloo. He organized and chaired numerous technical special sessions and tutorials in IEEE flagship conferences.

HILAL M. EL MISILMANI (Member, IEEE) was born in Beirut, Lebanon in 1987. He received the B.E. degree in communications and electronics engineering from Beirut Arab University, Lebanon, in 2010, and the M.E. and Ph.D. degrees in electrical and computer engineering from the American University of Beirut, Beirut, in 2012 and 2015, respectively.

From August 2011 to September 2012, he was a Telecommunications Engineer with Dar Al-Handasah Consultants (Shair and Partners). From September 2012 to August 2014, he was a Researcher with the Beirut Research and Innovation Center. From September 2014 to May 2015, he was a Lecturer with the American University of Beirut. From June 2015 to September 2016, he was a Research Associate with the American University of Beirut. Since September 2015, he has been an Assistant Professor with the Department of Electrical and Computer Engineering, Beirut Arab University. He is the author of more than 20 papers. His research interests include the design of high power microwave antennas, slotted waveguide antennas and Vlasov antennas, the design and applications of antenna arrays, antennas for biomedical applications, and machine learning in antenna design.

Dr. El Misilmani was a recipient of several scholarships, such as the Rafic Hariri Foundation Scholarship, from September 2005 to June 2010, the Association of Specialization and Scientific Guidance (SSG) Scholarship, from February 2006 to June 2010, the Lebanese Association for Scientific Research (LASeR) Scholarship, from September 2013 to May 2015, and the National Council for Scientific Research (CNRS) Doctoral Scholarship Award, from 2013 to May 2015.